Progress of Theoretical Physics, Vol. 53, No. 1, January 1975

Pinning Effect due to Periodic Variation of Impurity Concentration in Type II Superconductors

Seiju AMI and Kazumi MAKI*)

Department of Physics, Tohoku University, Sendai

(Received May 18, 1974)

By the use of Ginzburg-Landau equations, which include the effect arising from the sinusoidal variation of the impurity concentration in one direction, the stability of variety of the vortex lattice configuration in the type II superconductors is studied.

In the vicinity of the upper critical field H_{c2}, the critical current is determined as a function of the external field, which is compared with a recent experiment by Raffy et al. The present theory describes semi-quantitatively the observed field dependence of the critical current.

§ 1. Introduction

In spite of its practical importance, the pinning effect in the type II superconductors has been considered only within phenomenological model or in a statistical model until very recently. For example in a series of papers Yamafuji and his collaborators[1)~3)] have discussed the pinning effect within a model, which includes a phenomenological elastic coupling energy in addition to the ordinary Ginzburg-Landau free energy. More recently this type of model is taken up by Schmid and Hauger[4)] in order to consider the pinning effect on the moving vortex lines. On the other hand Larkin[5)] introduced a model with the spatial dependent Ginzburg-Landau (GL) coefficients in order to describe the pinning effect. The spatial inhomogeneities of the GL coefficients are characterized by the correlation function, which describes the spatial correlation of the inhomogeneity of the GL coefficients. Within this model Larkin studied the distortion of the vortex lattice from its equilibrium configuration in the pinning free sample. This model is further extended by Larkin and Ovchinikov[6)] to study the broadening of the structure in the density of states, the smearing of the transition temperature and so on due to the pinning centers.

The purpose of this work is twofold; we propose a very simple microscopic model which describes the pinning effect and we will study the stability of the vortex structure under uniform current within this model. The present model is motivated by a beautiful experimental work by Raffy et al.[7)] They prepared specimens of Pb-Bi alloys, where the Bi concentration is varied sinusoidally in

*) Now at Department of Physics, University of Southern California, Los Angeles, California 90007.

one direction. They studied the field dependence of the critical current which flows along the equiconcentration plane of the impurities and observed a remarkable structure in the critical current as a function of the external field. In accordance with their experimental situation, we adopt a model where the impurity concentration varies sinusoidally in one direction (say the y direction). The appropriate Ginzburg-Landau equations for this system are readily found for the dirty superconductors, when the spatial variation of the impurity concentration is sufficiently slow (i.e., the period of the variation a is longer than the electron mean free path l of the system). This is because nonmagnetic impurities affect hardly the transition temperature or other thermodynamical properties but the diffusion constant.[8] A somewhat related but different model from ours has been considered previously by Kulik and Itskovich,[9] who assumed that the pinning effect arises from the inhomogeneity in the concentration of magnetic impurities.

In the vicinity of the upper critical field, the most stable configuration is determined among the Abrikosov solutions[10] with doubly periodic structure. In general, the stable solution admits nonvanishing current along the equiconcentration plane of impurities in sharp contrast to the ideal case with no inhomogeneity where the transport current vanishes identically in the vortex state. The critical current is determined as the largest current the vortex state carries in the given configuration. The critical current takes the maximum values for the field $B_\triangle$, for which the period of the equilateral vortex lattice matches with the period of the impurity concentration.

The results are compared with the experiment by Raffy et al.[9] The present theory appears to describe semi-quantitatively the field dependence of the observed critical current at least in the high field region.

§ 2. Presentation of model

We will construct the Ginzburg-Landau free energy, which applies to the system with a periodic variation of the impurity concentration. We will limit ourselves to dirty superconductors for simplicity. For a dirty superconductor the free energy in the vicinity of the transition temperature T_c is given by[8]

$$\Omega_{SN}=\int d\boldsymbol{r}\Big[N(0)\Big\{-\frac{T_c-T}{T_c}|\Delta(\boldsymbol{r})|^2+\frac{7\zeta(3)}{16(\pi T_c)^2}|\Delta(\boldsymbol{r})|^4 +\frac{\pi}{8T_c}D|(\boldsymbol{\nabla}-2ie\boldsymbol{A})\Delta(\boldsymbol{r})|^2\Big\}+\frac{h^2(\boldsymbol{r})}{8\pi}\Big], \tag{1}$$

where $N(0)$ is the state density at the Fermi level, $\Delta(\boldsymbol{r})$ is the spatially dependent superconducting order parameter, D is the diffusion constant, $h(\boldsymbol{r})$ is the local magnetic field and $\zeta(z)$ is Riemann's zeta function. Three parameters $N(0)$, T_c and D characterize the system completely. Since the diffusion constant D is proportional to the transport life time τ_{tr},[8] only D can have a significant spatial dependence due to the inhomogeneity in the impurity concentration, while T_c and $N(0)$ are almost unchanged, if the impurity atom is nonmagnetic and chemically similar to the host atom. Furthermore, when the spatial variation in the impurity concentration is much slow (i.e., the period of the variation is longer than the electron mean free path l), the transport ilfe time is essentially inversely proportional to the impurity concentration $c_{\rm imp}(\boldsymbol{r})$

$$c_{\rm imp}(\boldsymbol{r}) = c_0\left(1+\Gamma \sin\left(\frac{2\pi}{a}y\right)\right) \qquad \text{with } \Gamma \geq 0 . \tag{2}$$

Here we have assumed that the impurity concentration varies in the y direction.

Therefore we will take the spatially dependent diffusion constant $D(\boldsymbol{r})$ to be

$$\begin{aligned} D(\boldsymbol{r}) &= D_0\left\{1+\Gamma \sin\left(\frac{2\pi}{a}y\right)\right\}^{-1} \\ &= \frac{D_0}{\sqrt{1-\Gamma^2}}\left\{1+2\sum_{\nu=1}^{\infty}(-g)^{\nu}\cos\left(\nu\left(\frac{2\pi}{a}y-\frac{\pi}{2}\right)\right)\right\} \end{aligned} \tag{3}$$

and

$$g = \Gamma(1+\sqrt{1-\Gamma^2})^{-1} . \tag{4}$$

Then the third term in the integrand in Eq. (1) is replaced by

$$N(0)\frac{\pi}{8T_c}D(\boldsymbol{r})\,|(\nabla - 2ie\boldsymbol{A})\Delta(\boldsymbol{r})|^2. \tag{5}$$

Since the coherence length ξ, the penetration depth δ and the Ginzburg-Landau parameter $\kappa = \delta/\xi$ are expressed in terms of $D(\boldsymbol{r})$ as

$$\xi = \left[\frac{\pi D(\boldsymbol{r})}{8(T_c - T)}\right]^{1/2},$$

$$\delta = \frac{1}{4e\pi^2}\left[\frac{7\zeta(3)}{2N(0)\,(T_c - T)\,D(\boldsymbol{r})}\right]^{1/2}$$

and

$$\kappa = \frac{1}{2e\pi^2 D(\boldsymbol{r})}\left[\frac{7\zeta(3)}{\pi N(0)}\right]^{1/2}, \tag{6}$$

respectively, ξ, δ and κ vary spatially in the present model.

Following Ginzburg and Landau[11] we will introduce a system of reduced units in order to simplify the subsequent analysis:

$$\boldsymbol{r}' = \boldsymbol{r}/\delta_0 ,$$

$$\boldsymbol{h}' = \boldsymbol{h}/\sqrt{2}H_c ,$$

$$\Delta' = \Delta\Big/\left[\frac{8(\pi T_c)^2}{7\zeta(3)}\left(1-\frac{T}{T_c}\right)\right],$$

$$j' = j \Big/ \frac{\sqrt{2}H_c}{4\pi\delta_0},$$

$$\mathcal{F}' = \mathcal{F} \Big/ \frac{H_c^2}{4\pi}\delta_0^3, \tag{7}$$

where

$$\delta_0 = \frac{1}{4e\pi^2}\left[\frac{7\zeta(3)}{2N(0)(T_c - T)D_0}\right]^{1/2}. \tag{8}$$

The free energy Ω_{SN} is now rewritten as

$$\mathcal{F}_{SH} \Big/ \frac{H_c^2}{4\pi} (\equiv F'V)$$

$$= \int dr \left[\frac{1}{2} - |\Delta'|^2 + \frac{1}{2}|\Delta'|^4 + h'^2 + \frac{1}{1+\Gamma\sin(2\pi y'/a')}\left|\left(\frac{\nabla'}{i\kappa_0} - A'\right)\Delta'\right|^2\right], \tag{9}$$

where

$$\kappa_0 = (2e\pi^2 D_0)^{-1}\left(\frac{7\zeta(3)}{\pi N(0)}\right)^{1/2} \tag{10}$$

and V is the volume of the specimen.

Ginzburg-Landau equations follow from the above free energy by taking a functional derivative by $\delta\Delta'$ or $\delta A'$

$$\left\{\left(\frac{\nabla}{i\kappa_0} - A\right)\frac{1}{1+\Gamma\sin(2\pi y/a)}\left(\frac{\nabla}{i\kappa_0} - A\right) - 1 + |\Delta|^2\right\}\Delta = 0 \tag{11}$$

and

$$j = \frac{1}{2}\frac{1}{1+\Gamma\sin(2\pi y/a)}\left\{\Delta^*\left(\frac{\nabla}{i\kappa_0} - A\right)\Delta + \text{c.c.}\right\}, \tag{12}$$

where we have taken off prime signs on Δ, A, ∇, a and y. The above set of equations reduce to the ordinary GL equations when $\Gamma = 0$.

§ 3. Variational solutions

We will look for solutions of Eqs. (11) and (12) in the presence of magnetic field H along the z axis. However, since the exact solution is known only in the vicinity of the upper critical field H_{c2} even in the homogeneous case (i.e., $\Gamma = 0$), we will limit our consideration in the vicinity of H_{c2}, where the order parameter is small. For the homogeneous system (or the ideal system), it is well known that the vortex array with the equilateral triangular lattice yields the lowest free energy.[12] However, in the presence of inhomogeneity the vortex lattice is likely to be deformed from the equilateral triangular structure.

In order to find out the most stable solution in the presence of the periodic variation of the impurity concentration, we resort to a variational approach. As a trial function we choose the Eilenberger vortex lattice (EVL) function,[13] which is a generalization of the Abrikosov solution for the homogeneous system at $H=H_{c2}$.

The EVL functions are defined by

$$\varphi_0(\boldsymbol{r}) = \left(\frac{2\eta}{b^2}\right)^{1/4} e^{-(\pi/\eta)y^2}\,\vartheta_3\left(\pi\frac{z}{b}\,\middle|\,\frac{\tau}{b^2}\right), \tag{13}$$

$$\varphi_n(\boldsymbol{r}) = \left[\left(\frac{4\pi}{\eta}\right)^n n!\right]^{-1/2} F_+^n \varphi_0(\boldsymbol{r}), \tag{14}$$

where

$$\boldsymbol{r}=(x,y),\ \eta=\frac{2\pi}{\kappa_0 B},\quad \text{(i.e., unit cell area)}$$

$$z=x+iy\,,\quad \tau=\zeta+i\eta\,,$$

$$F_\pm = i^{-1}\frac{\partial}{\partial x}+\frac{2\pi}{\eta}y\mp\frac{\partial}{\partial y}\,,$$

$$\vartheta_3(z|\tau) = \sum_{p=-\infty}^{\infty}\exp(2pzi+\pi\tau p^2 i), \tag{15}$$

(Riemann's theta function)

and B is magnetic induction. Furthermore EVL functions satisfy the following eigenvalue equation and the orthogonality condition

$$\left(\frac{\nabla}{i\kappa_0}-\boldsymbol{A}_0\right)^2\varphi_n = \frac{1}{\kappa_0^2}\left(F_+F_- + \frac{2\pi}{\eta}\right)\varphi_n = \varepsilon_n\varphi_n$$

and

$$\left(\int \varphi_n^*\varphi_m d^2r\right)\Big/\int d^2r = \delta_{nm}\,,$$

where

$$\boldsymbol{A}_0 = -\hat{x}By\,,$$

$$\varepsilon_n = \frac{2\pi}{\kappa_0^2\eta}(2n+1),\quad n=0,1,2,\cdots \tag{16}$$

and $\hat{x}$ is a unit vector in the x direction. The EVL function φ_0 describes a two-dimensional vortex lattice in the x-y plane with unit flux quantum per primitive cell. It is periodic with the periods given by

$$\boldsymbol{r}_1=(b,0)\quad\text{and}\quad \boldsymbol{r}_2=b^{-1}(\zeta,\eta).$$

Since we are going to calculate the transport current in the static vortex lattice, we will look for the solution of the linearized equation for $\Delta(\boldsymbol{r})$ within

$$\varphi=\varphi_0(\boldsymbol{r})+w\varphi_1(\boldsymbol{r}). \tag{17}$$

In fact we will see later that the mixing term ($\propto w$) contributes to the supercurrent of the order of Γ, while the mixing terms between φ_0 and φ_n with $n>1$ contribute to the supercurrent only higher order terms in Γ. When the induction B changes, the vortex lattice will be not only displaced and distorted but also rotated around the z axis to find the most stable solution. However, the base of a parallelogram of an elementary vortex lattice cell described by a function φ_0 is always along the x axis. Therefore in order to consider the vortex lattice configuration in full generality, we will rotate instead the configuration related to the spatial variation of the impurity concentration as shown in Fig. 1; we assume that the impurity concentration varies along the direction designated by $\boldsymbol{q}_0$, where

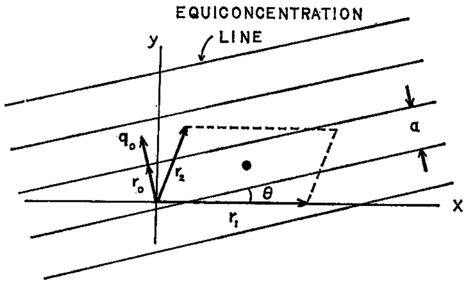

Fig. 1. The configuration of the unit cell of the vortex lattice to the equiconcentration line of impurities is shown. The lattice vectors of the unit cell are denoted by $\boldsymbol{r}_1$ and $\boldsymbol{r}_2$. The position of the center of vortex line is shown by the full circle.

$$\boldsymbol{q}_0=\frac{2\pi}{a}(-\sin\theta,\cos\theta),\quad 0\leq\theta<\pi, \tag{18}$$

$$D(\boldsymbol{r})=\frac{D_0}{\sqrt{1-\Gamma^2}}[1-2g\sin\boldsymbol{q}_0\cdot(\boldsymbol{r}-\boldsymbol{r}_0)] \tag{19}$$

and

$$\boldsymbol{r}_0/\!/\boldsymbol{q}_0,\qquad 0\leq r_0<a.$$

Here we have neglected the higher order terms in g for simplicity. We will now solve the linearized equation for Δ variationally:

$$\left(\frac{\nabla}{i\kappa_0}-\boldsymbol{A}_0\right)\frac{1}{\sqrt{1-\Gamma^2}}[1-2g\sin\boldsymbol{q}_0\cdot(\boldsymbol{r}-\boldsymbol{r}_0)]\left(\frac{\nabla}{i\kappa_0}-\boldsymbol{A}_0\right)\Delta=E_0\Delta \tag{20}$$

with the smallest E_0, where $\boldsymbol{A}_0$ is taken to be

$$\boldsymbol{A}_0=-\hat{x}By. \tag{21}$$

We can convert Eq. (20) into a variational equation

$$E_0=\frac{\int d^2r\{(1/\sqrt{1-\Gamma^2})(1-2g\sin\boldsymbol{q}_0\cdot(\boldsymbol{r}-\boldsymbol{r}_0))\,|(\nabla/i\kappa_0-\boldsymbol{A}_0)\Delta|^2\}}{\int d^2r|\Delta|^2}. \tag{22}$$

Substituting $\Delta=C\varphi$ in Eq. (22), where φ is defined by Eq. (17), we have (see the Appendix for details);

$$E_0=\frac{B}{\tilde{\kappa}_0}\left(1+2g\left(1-\frac{\eta}{4\pi}q_0^2\right)\exp\left(-\frac{\eta}{8\pi}q_0^2\right)\right.$$
$$\left.\times\sin(\boldsymbol{q}_0\cdot\boldsymbol{r}_0)(-1)^{mn}\delta\left(\frac{b}{a}\sin\theta,m\right)\delta_1\left(\frac{\eta}{a}\cos\theta-\frac{\zeta}{a}\sin\theta,n\right)\right] \quad (23)$$

with

$$w=g\left(\frac{\eta}{4\pi}\right)^{1/2}q_0\left\{\left(1-\frac{\eta}{4\pi}q_0^2\right)e^{i\theta}+e^{-i\theta}\right\}\exp\left(-\frac{\eta}{8\pi}q_0^2\right)$$
$$\times\cos(\boldsymbol{q}_0\cdot\boldsymbol{r}_0)(-1)^{mn}\delta\left(\frac{b}{a}\sin\theta,m\right)\delta_1\left(\frac{\eta}{a}\cos\theta-\frac{\zeta}{a}\sin\theta,n\right), \quad (24)$$

where

$$\tilde{\kappa}_0=\kappa_0(1-\Gamma^2)^{1/2}, \quad (25)$$

$$\delta(x,m)=\begin{cases}1 & \text{for } x=m,\ (m\text{: integer})\\ 0 & \text{otherwise}\end{cases} \quad (26)$$

and

$$\delta_1(x,n)=\frac{\eta}{bL_y}\sum_{P=-L_yb/(2\eta)}^{L_yb/(2\eta)}\cos\left(\frac{2\pi}{b}px\right)=\frac{\eta\sin[(2\pi/b)(L_yb/2\eta+1/2)x]}{bL_y\sin((\pi/b)x)}$$
$$\rightarrow\begin{cases}1 & \text{for } x=bn,\ (x\text{: integer})\\ 0 & \text{otherwise}\end{cases} \quad (27)$$

when L_yb/η tends to infinity. The above eigenvalue E_0 is exact to first order in g. We note also that E_0 gives the upper critical field of the system under consideration.

The normalization constant C of the order parameter is determined by following the original procedure due to Abrikosov.[10] For this purpose we have to first determine the local field $\boldsymbol{h}$;

$$\nabla\times(\nabla\times\boldsymbol{h})=\boldsymbol{j}[\boldsymbol{A}_0,\Delta]. \quad (28)$$

Introducing $\boldsymbol{h}_1$ by

$$\boldsymbol{h}=\boldsymbol{B}+\boldsymbol{h}_1, \quad (29)$$

we have

$$\boldsymbol{h}_1=-\frac{1}{2\tilde{\kappa}_0}[\{1-2g\sin\boldsymbol{q}_0\cdot(\boldsymbol{r}-\boldsymbol{r}_0)\}|\Delta|^2$$
$$-\langle\{1-2g\sin\boldsymbol{q}_0\cdot(\boldsymbol{r}-\boldsymbol{r}_0)\}|\Delta|^2\rangle]\hat{z} \quad (30)$$

and

$$\langle\boldsymbol{h}\rangle=\boldsymbol{B},$$

where $\langle A\rangle$ denotes the space average of A. In the above calculation, we have neglected a part of $\boldsymbol{j}[\boldsymbol{A}_0,\Delta]$, which gives rise to a macroscopic transport current. Within the present approximation this current is not divergent free, although a more careful treatment[14] of the back flow term will make this term divergent free as required from the current conservation.

The amplitude of Δ is then determined from

$$\left\langle \Delta^*\left[\left(\frac{\nabla}{i\kappa_0}-A\right)(1-\Gamma^2)^{-1/2}\{1-2g\sin q_0\cdot(r-r_0)\}\left(\frac{\nabla}{i\kappa_0}-A\right)\right.\right.$$
$$\left.\left. -1+|\Delta|^2\right]\Delta\right\rangle=0\,, \tag{31}$$

where

$$A=A_0+A_1 \quad \text{and} \quad \nabla\times A_1=h_1\,. \tag{32}$$

Substituting the expression for $\Delta(\equiv C\varphi)$ into Eq. (31) we obtain

$$|C|^2=\frac{2\tilde{\kappa}_0^2(1-E_0)}{1+\alpha+\beta_A(2\tilde{\kappa}_0^2-1-\alpha')}\,, \tag{33}$$

where

$$\alpha=-4g\langle\sin[q_0\cdot(r-r_0)]|\varphi_0|^2\rangle$$
$$=4g\exp\left(-\frac{q_0^2}{8\pi}\eta\right)\sin(q_0\cdot r_0)(-1)^{mn}\delta\left(\frac{b}{a}\sin\theta,m\right)$$
$$\times\delta_1\left(\frac{\eta}{a}\cos\theta-\frac{\zeta}{a}\sin\theta,n\right),$$
$$\alpha'=-4g\langle\sin[q_0\cdot(r-r_0)]|\varphi_0|^4\rangle/\beta_A$$
$$=4g\exp\left(-\frac{q_0^2}{8\pi}\frac{\eta}{2}\right)\sin(q_0\cdot r_0)(-1)^{mn}\delta\left(\frac{b}{a}\sin\theta,m\right)$$
$$\times\frac{1}{2}\delta_1\left(\frac{\eta}{2a}\cos\theta-\frac{\zeta}{2a}\sin\theta,n\right)$$

and

$$\beta_A=\langle|\Delta|^4\rangle/\langle|\Delta|^2\rangle^2. \tag{34}$$

Putting

$$X=\frac{\zeta^{1/2}}{b} \quad \text{and} \quad Y=\frac{\eta^{1/2}}{b}\,,$$

we have

$$\beta_A=Y\sum_{p,q=-\infty}^{\infty}\cos(2\pi X^2pq)\exp[-\pi Y^2(p^2+q^2)]. \tag{35}$$

Finally the free energy and the transport current $\langle j\rangle$ are given as

$$F=\frac{1}{2}+B^2-\frac{\tilde{\kappa}_0^2(1-E_0)^2}{1+\alpha+\beta_A(2\tilde{\kappa}_0^2-1-\alpha')} \tag{36}$$

and

$$\langle \boldsymbol{j} \rangle = g\frac{1}{\tilde{\kappa}_0}\boldsymbol{q}_0\left(1-\frac{q_0^2}{4\pi}\eta\right)\exp\left(-\frac{q_0^2}{8\pi}\eta\right)\cos(\boldsymbol{q}_0\cdot\boldsymbol{r}_0)$$

$$\times(-1)^{mn}\delta\left(\frac{b}{a}\sin\theta, m\right)\delta_1\left(\frac{\eta}{a}\cos\theta-\frac{\zeta}{a}\sin\theta, n\right)$$

$$\times\frac{2\tilde{\kappa}_0^2(1-E_0)}{1+\alpha+\beta_A(2\tilde{\kappa}_0^2-1-\alpha')}(\hat{x}\cos\theta+\hat{y}\sin\theta), \qquad (37)$$

respectively.

It is of interest to note that the current equation (37) satisfies the force balance equation:[15]

$$\nabla_{r_0}F+2\langle \boldsymbol{j}\rangle\times\boldsymbol{B}=0, \qquad (38)$$

if we neglect the higher order terms in $(1-E_0)$. Since the second term is the Lorentz force term, we can identify the first term as the pinning force term. Therefore the present model gives rise to a pinning force in the direction parallel to the concentration variation of impurities. We also point out that the pinning force arises only when the period of the vortex lattice is commensurate with the period of the concentration variation;

$$\begin{cases}\boldsymbol{q}_0\cdot\boldsymbol{r}_1=-2\pi m, \\ \boldsymbol{q}_0\cdot\boldsymbol{r}_2=-2\pi n,\end{cases} \qquad (39)$$

and n, m are integers. On the other hand, when the vortex lattice does not fullfil the above condition, the term proportional to g in the free energy has no effect on the vortex lattice within the present approximation and F and $\langle \boldsymbol{j}\rangle$ reduce to those obtained by Abrikosov[10] previously:

$$F^0=\frac{1}{2}+B^2-\frac{(\tilde{\kappa}_0-B)^2}{1+\beta_A^0(2\tilde{\kappa}_0^2-1)}, \qquad (40)$$

$$\langle \boldsymbol{j}\rangle=0$$

with $\beta_A^0=1.16$.

§ 4. Commensurate solution

In this section, we will summarize the properties of the commensurate solution which satisfies the condition (39). In particular, when the commensurate solution has an equilateral triangular vortex lattice, we will expect the largest critical current. Therefore we will study first this resonance condition.

a) *The resonance condition*

The resonance condition is satisfied when the induction B takes particular values B_Δ. Since we are interested in an equilateral triangular lattice, we have

$$\begin{cases} b = ((2/\sqrt{3})\eta)^{1/2}, \\ \zeta/b = b/2\,. \end{cases}$$

Substituting the above relations into Eq. (39), we obtain

$$B_\triangle = \frac{\sqrt{3}\pi}{a^2\kappa_0}(n^2+m^2+nm)^{-1}$$
$$= \frac{\sqrt{3}}{2a^2}\phi_0(n^2+m^2+nm)^{-1} \quad \text{(in the natural unit)} \tag{41}$$

and

$$\sin\theta = \frac{m}{2}\left(\frac{3}{n^2+m^2+nm}\right)^{1/2}, \tag{42}$$

where $\phi_0 = hc/2e$ is the unit flux. Since $B_\triangle$ is expressed in terms of a only (in the natural unit), we believe the above result holds independent of the details of the model employed. We note also that the resonance solutions are in general multiply degenerated, since there are a number of pairs (n, m), which make up the same (n^2+m^2+nm). This degeneracy arises partly from the nonuniqueness in choosing unit vectors describing a regular triangular lattice and partly from the existence of the reflected solution on the plane parallel to $\boldsymbol{q}_0$, if the solution does not have the reflection symmetry. The resonance field $B_\triangle$ and the corresponding unit cell of the vortex lattice are shown in Table I. The parallel lines indicate the equiconcentration plane of impurities with a period a. The field $B_\triangle$ takes the following series of numbers

$$\frac{2a^2}{\sqrt{3}}B_\triangle/\phi_0 = 1,\ \frac{1}{3},\ \frac{1}{4},\ \frac{1}{7},\ \frac{1}{9},\ \frac{1}{12},\ \cdots.$$

b) *The upper critical field H_{c2}*

The upper critical field is defined as the magnetic field, which satisfies

$$E_0 = 1\,, \tag{43}$$

where E_0 has been already defined by Eq. (23). In the case of incommensurate solution, Eq. (43) yields

$$H_{c2}^0 = \tilde{\kappa}_0 \tag{44}$$

as in the Abrikosov theory. For a commensurate solution, on the other hand, we have

$$H_{c2}^0/H_{c2} = 1 + 2gQ(H_{c2})\sin(\boldsymbol{q}_0\cdot\boldsymbol{r}_0) \tag{45}$$

with

$$Q(x) = \left(1 - \frac{2\pi^2}{a^2\kappa_0 x}\right)\exp\left(-\frac{\pi^2}{a^2\kappa_0 x}\right). \tag{46}$$

Table I.

$\frac{2a^2}{\sqrt{3}\,\phi_0}B_\Delta$	(m, n)	Vortex lattice cotiguration
1	(0, 1)	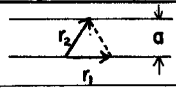
$\frac{1}{3}$	(2, −1)	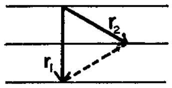
$\frac{1}{4}$	(0, 2)	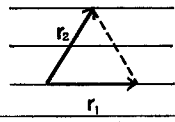
$\frac{1}{7}$	(i) (ii) (1, 2), (3, −2)	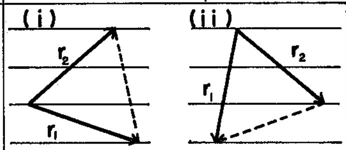
$\frac{1}{9}$	(0, 3)	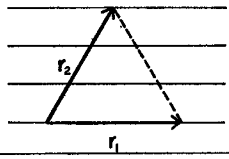
$\frac{1}{12}$	(4, −2)	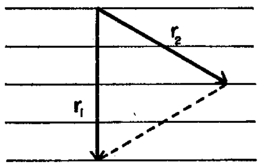

Here we limit ourselves to the case $m=0$, which is of particular importance in the following analysis.

We will have $H_{c2} \geq H^0_{c2}$, only when the second term in the r.h.s. is negative. This yields for the largest H_{c2},

$$\sin(\boldsymbol{q}_0 \cdot \boldsymbol{r}_0) = \begin{cases} -1 & \text{for} \quad a > (2\pi^2/\kappa_0 H_{c2})^{1/2}, \\ \;\;\,1 & \text{for} \quad a < (2\pi^2/\kappa_0 H_{c2})^{1/2}. \end{cases} \tag{47}$$

This result implies that, when $a < (2\pi^2/\kappa_0 H_{c2})^{1/2}$, the nucleation of superconductivity starts at the trough in κ (i.e., in the region of dilute concentration of impurity), while, when $a > (2\pi^2/\kappa_0 H_{c2})^{1/2}$, it starts at the crest of κ. This is because an islet of the nucleated superconductivity has a spatial extension of the order of

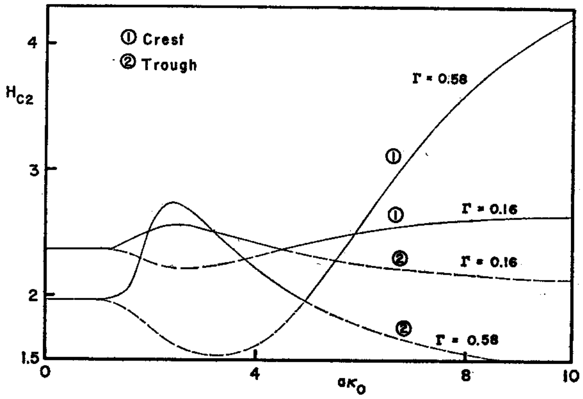

Fig. 2. The upper critical fields associated with the commensurate solution are shown as function of $\kappa_0 a$. Crest and trough on the curves indicates the branches of solutions with the center of superconducting islet at the crest and at the trough of the impurity concentration.

$(2\pi^2/\kappa_0 H_{c2})^{1/2}$. The upper critical field given by Eq. (45) is calculated numerically and shown in Fig. 2 for some values of the Γ's as functions of $\kappa_0 a$. The critical field H_{c2} has a prominent peak around $\kappa_0 a \simeq 2$ and becomes H^0_{c2} for $a = (2\pi^2/\kappa_0 H_{c2})^{1/2}$. Furthermore, H_{c2} exhibits the following asymptotic behavior

$$\begin{aligned} H_{c2} &\simeq H^0_{c2} && \text{for} \quad a \ll (2\pi^2/\kappa_0 H^0_{c2})^{1/2}, \\ &\cong (1+2g) H^0_{c2} && \text{for} \quad a \gg (2\pi^2/\kappa_0 H^0_{c2})^{1/2}. \end{aligned} \tag{48}$$

As the temperature decreases, a in the reduced unit (we write it a' here) increases according to

$$a' = 4e\pi^2 a \left[\frac{7\zeta(3)}{2N(0)(T_c - T)D_0}\right]^{-1/2}. \tag{49}$$

Therefore we can pass to the one region to the another by simply changing the temperature. The upper critical field in conventional units is given as

$$8\pi(T_c - T)\left[\frac{2\pi N(0)}{7\zeta(3)}\right]^{1/2} \frac{\tilde{\kappa}_0}{H_{c2}} = 1 + 2gQ(H_{c2})\sin(\boldsymbol{q}_0 \cdot \boldsymbol{r}_0), \tag{50}$$

where Q is now expressed as

$$Q(x) = \left(1 - \frac{\pi\phi_0}{a^2 x}\right)\exp\left(-\frac{\pi\phi_0}{2a^2 x}\right). \tag{51}$$

The temperature dependence of $H_{c2}(T)$ is shown in Fig. 3 for particular values of a.

c) *Free energy density*

The free energy density of a commensurate solution is given by

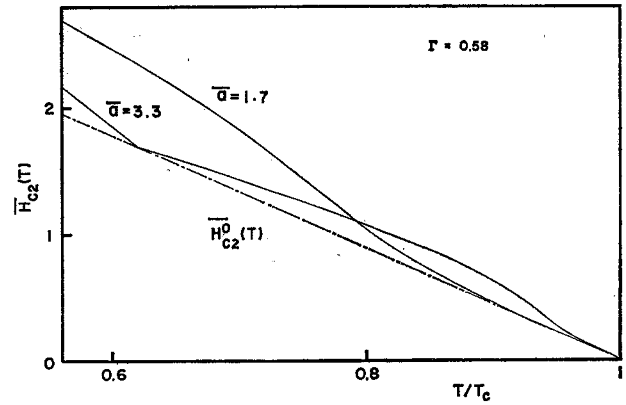

Fig. 3. The temperature dependence of the upper critical field for the commensurate solution is shown. The critical field H_{c2} and the period a are scaled by $\sqrt{2}\bar{H}_c = -\sqrt{2}T_c(dH_c/dT)_{T=T_c}$ and $\bar{\delta}_0 = (1-T/T_c)^{1/2}\delta_0$, respectively.

$$F = \frac{1}{2} + B^2 - \frac{1}{1+\beta_A(2\tilde{\kappa}_0^2 - 1)}[\tilde{\kappa}_0 - B\{1 + 2gQ(B)\sin(\boldsymbol{q}_0 \cdot \boldsymbol{r}_0)\}]^2, \tag{52}$$

where we have discarded small terms α and α' in Eq. (36). Furthermore we confine ourselves to the special class of solutions with $m=0$, which appears to be relevant to the experiments. The lowest free energy is obtained, for the configuration with the largest H_{c2} (or with the smallest H_{c2} when the sign of Q is reversed for given B from the one at $B=H_{c2}$) and with the smallest β_A. The first condition is readily satisfied if we take $\sin(\boldsymbol{q}_0 \cdot \boldsymbol{r}_0)$ defined by Eq. (47), although now H_{c2} in Eq. (47) has to be replaced by B. In order to compute β_A, on the other hand, we have to specify further the vortex lattice configuration. Since we took already ($m=0$), we look for a solution with a base of the vortex lattice parallelogram on the equiconcentration plane. In this case we have

$$m=0\,, \quad \frac{\eta}{b} = an\,, \quad Y = \frac{\eta^{1/2}}{b} = an\left(\frac{\kappa_0 B}{2\pi}\right)^{1/2} \tag{53}$$

and

$$X^2 = \frac{1}{2}$$

since the smallest β_A is obtained when the parallelogram consists of two isosceles. Then β_A is given by

$$\beta_A = an\left(\frac{\kappa_0 B}{2\pi}\right)^{1/2} \sum_{p,q=-\infty}^{\infty} \cos(\pi pq) \exp\left(-a^2 n^2 \frac{\kappa_0 B}{2}(p^2+q^2)\right). \tag{54}$$

In particular in the vicinity of $B=B_\Delta$, β_A can be expanded in powers of $(Y - \sqrt{\sqrt{3}/2})$ as

$$\beta_A = \beta_A^0 + 1.101\left(Y - \sqrt{\frac{\sqrt{3}}{2}}\right)^2 + \cdots.$$

In order to decide if the commensurate solution is really stable, we have to compare the resultant free energy (52) with F^0 given by Eq. (40).

d) *The critical current* J_{cr}

The critical current J_{cr} is defined as the maximum supercurrent in the system. In the vortex state of an ideal system, there is always dissipation due to the flux flow whenever the transport current is applied. This implies $J_{cr}=0$ in the vortex state of the ideal system. However, in real superconductors, which in general contain some kind of inhomogeneities, flux lines are pinned to those inhomogeneities. This allows a non-dissipative transport current in the vortex state, until the current attains the critical value. In the present model the role of pinning centers is played by the spatial variation of the impurity concentration. As we have already seen a macroscopic supercurrent flows along the equiconcentration plane for the commensurate solutions.

$$\langle \boldsymbol{j} \rangle = \frac{\tilde{\kappa}_0^2}{1+\beta_A(2\tilde{\kappa}_0^2-1)}\left[1-\frac{B}{\tilde{\kappa}_0}\{1+2gQ(B)\sin(\boldsymbol{q}_0\cdot\boldsymbol{r}_0)\}\right] \times 2g\frac{1}{\tilde{\kappa}_0}q_0 Q(B)\cos(\boldsymbol{q}_0\cdot\boldsymbol{r}_0)\hat{x}\,. \tag{55}$$

We note that $\langle \boldsymbol{j} \rangle$ vanishes for the equilibrium $\boldsymbol{r}_0(=\boldsymbol{r}_{0e})$ given by Eq. (47). When the external current is applied parallel to the equiconcentration plane (i.e., along the x axis) the equilibrium vortex lattice moves in the y direction in order to balance the Lorentz force with the pinning force. Therefore the critical current is determined by the maximum pinning force arising from the periodic variation of the impurity concentration. However, at the same time the free energy of the commensurate solution with the current has to be still lower than the free energy of the incommensurate solution, if such a configuration is really stable; the commensurate solution has to satisfy

$$\frac{B}{\tilde{\kappa}_0}[1+2gQ(B)\sin(\boldsymbol{q}_0\cdot\boldsymbol{r}_0)] \le 1 \tag{56}$$

and

$$\Delta F = -\frac{1}{1+\beta_A(2\tilde{\kappa}_0^2-1)}[\tilde{\kappa}_0 - B\{1+2gQ(B)\sin(\boldsymbol{q}_0\cdot\boldsymbol{r}_{0e})\}]^2 + \frac{(\tilde{\kappa}_0-B)^2}{1+\beta_A^0(2\tilde{\kappa}_0^2-1)} \le 0\,. \tag{57}$$

When both Eqs. (56) and (57) are satisfied by the commensurate solution, the maximum value of Eq. (55) yields the critical current

$$J_{cr}=\frac{\tilde{\kappa}_0^2}{1+\beta_A(2\tilde{\kappa}_0^2-1)}\frac{q_0}{B}$$
$$\times\left\{\left[\frac{1}{16}\left(1-\frac{B}{\tilde{\kappa}_0}\right)^2+2\left(\frac{B}{\tilde{\kappa}_0}gQ(B)\right)^2\right]^{1/2}+\frac{3}{4}\left(1-\frac{B}{\tilde{\kappa}_0}\right)\right\}^{3/2}$$
$$\times\left\{\left[\frac{1}{16}\left(1-\frac{B}{\tilde{\kappa}_0}\right)^2+2\left(\frac{B}{\tilde{\kappa}_0}gQ(B)\right)^2\right]^{1/2}-\frac{1}{4}\left(1-\frac{B}{\tilde{\kappa}_0}\right)\right\}^{1/2}\hat{x}\,. \quad (58)$$

§ 5. Comparison with experiment

We will now compare our result with a recent experiment by Raffy et al.[7] They measured the field dependence of the critical current of the vortex state in Pb-Bi alloys, where the Bi concentration is varied periodically in one direction. The specimens they used have the following parameters

$$\kappa_0=2.4,\ \delta_0=850\text{Å}\quad\text{and}\quad H_c=600\text{ Oe}$$
$$\text{and}\quad \Gamma=0.16\quad\text{and}\quad 0.58$$

depending on the duration of annealing. The number deduced for Γ may be somewhat ambiguious, since we used the values of the maximum concentration and the minimum concentration for their specimens together with their relation between the electronic mean free path and the Bi concentration for a homogeneous specimen. Furthermore, since the specimens are not quite in the dirty limit (i.e., $l/\xi_0\sim 0.25$), we employed the Gor'kov expression for superconducting coherence length in alloys to obtain above Γ.

For the purpose of comparison, we have chosen four sets of experimental data for specimens (1) with $a=1.1$ (reduced unit) and $\Gamma=0.16$ or 0.58 and (2) with $a=2.2$ and $\Gamma=0.16$ or 0.58. The experimental configurations are shown in Figs. 4(a) and (b). We are interested here in the configuration (a). In the configuration (b) where $\boldsymbol{H}$ is perpendicular to the equiconcentration plane, the flux lines feel no pinning effect due to the periodic variation of the impurity concentration but may feel other pinning effect due to mainly uncontrollable defects. This leads to a monotonic decrease of J_{cr} as the magnetic field increases. In the following we will call other pinning effects, which are not related to the

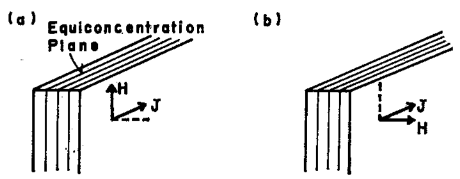

Fig. 4. The two experimental configurations are shown. In the configuration (a), where $\boldsymbol{H}$ is parallel to the equiconcentration plane, the pinning force due to the spatial variation of the impurity concentration is exerted on the vortex lattice, while in the configuration (b) the vortex lattice feels no pinning force.

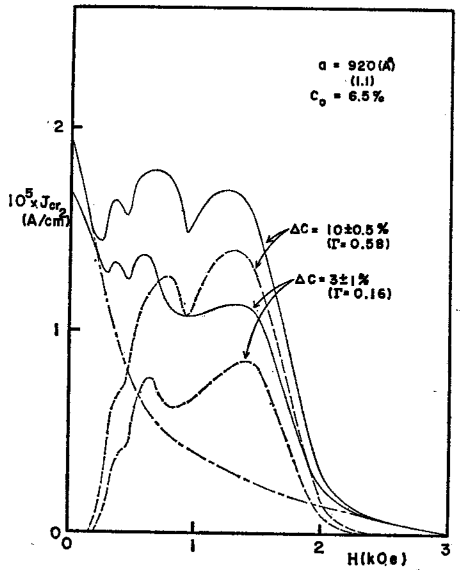

Fig. 5. The experimental data on the critical currents are shown as function of H for the sample with a=920Å. The broken curves are obtained from the critical currents by subtracting the residual one.

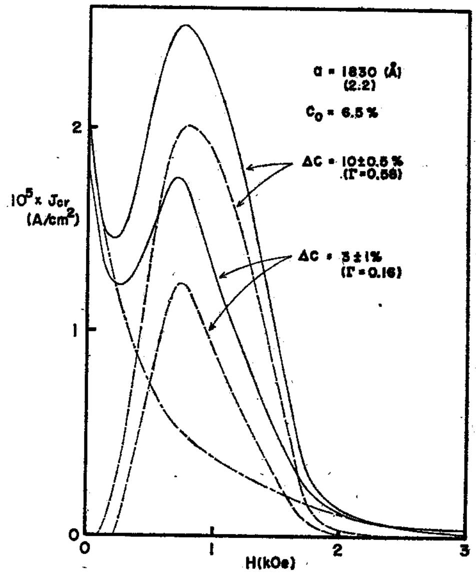

Fig. 6. The critical currents are shown as function of H for the sample with a=1830Å.

periodic variation of the impurity concentration the residual one. In the configuration (a), where the pinning effect due to the variation of impurity concentration plays an important role, the critical field is found to have characteristic peaks as shown in Figs. 5 and 6. However, the observed critical current contains still the component due to the residual pinning. Since we are interested only in the critical current associated with the periodic variation of the impurity concentration, it is necessary to subtract the critical current due to the residual pinning before any comparison is made.

As we have no experiment of the critical current in homogeneous sample, we constructed the critical current due to the residual pinning as shown by chained curve. Substracting the residual critical current thus determined from the observed critical current, we obtained the critical currents as shown by broken lines in Figs. 5 and 6.

First we will compare the peak position of the critical current with $B_\triangle$ the resonance magnetic field. For this purpose, it is necessary to calculate the corresponding $H_\triangle$, which we determined by using the Abrikosov formula:

$$H_\triangle = B_\triangle + \frac{\tilde{\kappa}_0 - B_\triangle}{1+\beta_A(2\tilde{\kappa}_0^2 - 1)}, \tag{59}$$

since the difference between this expression and the corresponding formula for

Table II.

a (reduced units)	Theory			Experiment	
	$B_\triangle$ (reduced units)	$H_\triangle$ (Oe)		H_{peak} (Oe)	
		$\Gamma=0.16$	$\Gamma=0.58$	$\Gamma=0.16$	$\Gamma=0.58$
1.1	1.87	1600	1600	1400	1300
	0.68	690	700	650	750
	0.47	520	540		
	0.25	350	380	400	400
2.2	0.47	520	540	740	760

the commensurate solution is extremely small (i.e., $\Delta F/F^0 \sim 10^{-2}$). However, it has to be borne in mind that Eq. (59) is valid only in the vicinity of $H \sim H_{c2}$. Experimental peaks of the critical current are determined from broken curves in Figs. 5 and 6 and shown in Table II. We note that there is fair correspondence between the theory and the experiment, although for the specimen with $a=2.2$, the theoretical peak appears in much lower field region. Furthermore in the specimen with $a=1.1$, the field $H_\triangle=350$ Oe gives no peak in the observed current but a simple shoulder. We also note that the peak corresponding $B_\triangle=0.47$ seems missing in the experiment. This may imply that the vortex lattice does not rotate much when the external field is changed, since $B_\triangle=0.47$ corresponds to the third configuration in Table I.

The critical current (Eq. (58)) and ΔF (given by Eq. (57)) are evaluated numerically and shown in Figs. 7 and 8 for the sample with $a=1.1$ and $a=2.2$, respectively. In the insert the field dependences of ΔF are shown. The theoretical curves (solid curves) are compared with the experimental curves (broken curves) which are taken from Figs. 5 and 6, respectively. For the specimen with $a=1.1$, the theoretical behavior of the critical current reproduces fairly well the experimental result in the high field region, although we have to multiply the theoretical value by $(22)^{-1}$ in order to get a reasonable fit. In lower field region, where our variational solution is a poor approximation to the order parameter, we cannot reproduce the large structure as observed in the experiment. For the specimen with $a=2.2$, the correspondence between the theory and the experiment become poorer. This is probably due to the fact that already the first peak in the critical current appears in a field much lower than H_{c2}.

Therefore we may conclude that the present model describes fairly well the observed critical current in the high field region (i.e., $H \sim H_{c2}$). However the theory predicts the critical current about a factor of 10 larger than the experimental value. It may be due to several origins. First we assumed that the impurity concentration varies as a sinusoidal function. Second, we deduced the value of Γ from the experimental data for the maximum concentration and the

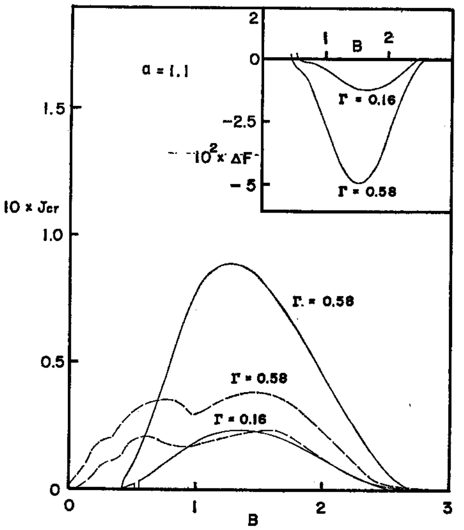

Fig. 7. The theoretical critical currents are shown for $a=1.1$ and $\Gamma=0.58$ and $\Gamma=0.16$ as function of the induction B. In the insert we plot the free energy difference ΔF for the commensurate solution and the incommensurate solution.

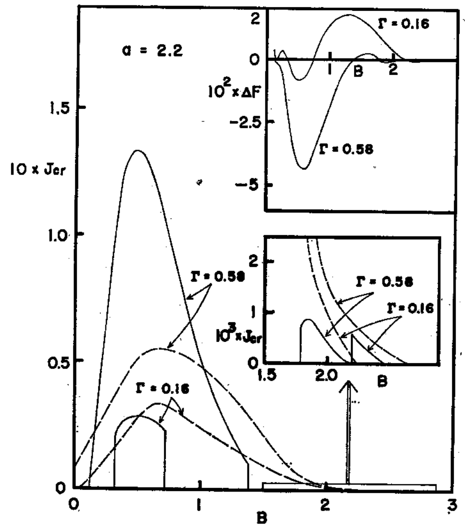

Fig. 8. The theoretical critical currents are shown for $a=2.2$ and $\Gamma=0.58$ and $\Gamma=0.16$.

minimum concentration, but we do not know the electron mean free paths for the corresponding concentrations. Furthermore we assumed that the system is infinite in size, while the experiment has been done in the system with the thickness of several μ's. More works on this subject are certainly desirable. After completion of this work, we became aware of a new work by Raffy et al.,[16] where they measured the temperature dependence of the critical current as function of magnetic field. A preliminary comparison seems to suggest that the present theory describes the observed temperature dependence of the critical current fairly well. The details of the analysis will be published elsewhere.

Acknowledgement

We are grateful to Dr. Hélène Raffy for providing us her Theses before publication, which motivated present study.

Appendix

We will calculate the following integral:

$$I=\int \sin \boldsymbol{q}_0\cdot(\boldsymbol{r}-\boldsymbol{r}_0)\left|\left(\frac{\nabla}{i\kappa_0}-\boldsymbol{A}_0\right)\varphi_0\right|^2 d^2r \Big/ \int d^2r\,, \qquad (\mathrm{A}\cdot 1)$$

where $\boldsymbol{A}_0=-\hat{x}By$ and φ_0 is defined by Eq. (13). Substituting φ_0 in (A1) and integrating over x, we have

$$I=2\left(\frac{2\eta}{b^2}\right)^{1/2}\left(\frac{2\pi}{\kappa_0\eta}\right)^2\frac{1}{2iL_y}\int_{-L_y/2}^{L_y/2}\sum_{p,q=-\infty}^{\infty}\delta\left(p-q-\frac{q_0b}{2\pi}\sin\theta,0\right)$$
$$\times\left(y+\frac{\eta}{b}p\right)\left(y+\frac{\eta}{b}q\right)\exp\left[iq_0\,y\cos\theta-\frac{2\pi}{\eta}y^2-\frac{2\pi}{b}(p+q)y\right.$$
$$\left.+\frac{\pi}{b^2}i(p^2-q^2)\zeta-\frac{\pi}{b^2}(p^2+q^2)\eta-i\boldsymbol{q}_0\cdot\boldsymbol{r}_0\right]-(q_0\rightarrow-q_0). \qquad (\text{A}\cdot 2)$$

Furthermore we can carry out the summation over q, which yields

$$I=2\left(\frac{2\eta}{b^2}\right)^{1/2}\left(\frac{2\pi}{\kappa_0\eta}\right)^2\frac{1}{2i}\sum_{p,q=-\infty}^{\infty}\frac{1}{L_y}\int_{-L_y/2}^{L_y/2}dy\left(y+\frac{\eta}{b}p\right)\left(y+\frac{\eta}{b}p-\frac{\eta}{2\pi}q_0\sin\theta\right)$$
$$\times\exp\left[-\frac{2\pi}{\eta}\left\{y+\frac{\eta}{b}\left(p-i\frac{b}{4\pi}q_0e^{-i\theta}\right)\right\}^2+i\frac{q_0}{b}p(\zeta\sin\theta-\eta\cos\theta)\right.$$
$$\left.-\frac{q_0^2}{8\pi}\eta+i\frac{q_0^2}{4\pi}\sin\theta(\eta\cos\theta-\zeta\sin\theta)-i\boldsymbol{q}_0\cdot\boldsymbol{r}_0\right]\delta\left(\frac{b}{a}\sin\theta,m\right)-(q_0\rightarrow-q_0)$$
$$(\text{A}\cdot 3)$$
$$=2\left(\frac{2\eta}{b^2}\right)^{1/2}\left(\frac{2\pi}{\kappa_0\eta}\right)^2\frac{1}{2iL_y}\sum_{p=-L_yb/(2\eta)}^{L_yb/(2\eta)}\int_{-\infty}^{\infty}dy\left(y+i\frac{\eta}{4\pi}q_0e^{-i\theta}\right)$$
$$\times\left(y+i\frac{\eta}{4\pi}q_0e^{-i\theta}-\frac{\eta}{2\pi}q_0\sin\theta\right)\exp\left[-\frac{2\pi}{\eta}y^2\right.$$
$$+i\frac{q_0}{b}p(\zeta\sin\theta-\eta\cos\theta)-\frac{\eta}{8\pi}q_0^2+i\frac{q_0^2}{4\pi}\sin\theta(\eta\cos\theta-\zeta\sin\theta)$$
$$\left.-i\boldsymbol{q}_0\cdot\boldsymbol{r}_0\right]\delta\left(\frac{b}{a}\sin\theta,m\right)$$
$$-(q_0\rightarrow-q_0). \qquad (\text{A}\cdot 4)$$

In going from (A·3) to (A·4), we made use of the transformation

$$\sum_{p=-\infty}^{\infty}\int_{-L_y/2}^{L_y/2}\rightarrow\sum_{p=-L_yb/(2\eta)}^{L_yb/(2\eta)}\int_{-\infty}^{\infty} \qquad (\text{A}\cdot 5)$$

which is allowable thanks to the exponential factor in the integrand. Finally the integration over y yields

$$I=-\frac{B}{\kappa_0}\sin(\boldsymbol{q}_0\cdot\boldsymbol{r}_0)\left(1-\frac{\eta}{4\pi}q_0^2\right)\exp\left(-\frac{\eta}{8\pi}q_0^2\right)$$
$$\times(-1)^{mn}\delta\left(\frac{b}{a}\sin\theta,m\right)\delta_1\left(\frac{\eta}{a}\cos\theta-\frac{\zeta}{a}\sin\theta,n\right). \qquad (\text{A}\cdot 6)$$

References

1) F. Irie and K. Yamafuji, J. Phys. Soc. Japan **23** (1967), 255.
2) K. Miyahara, F. Irie and K. Yamafuji, J. Phys. Soc. Japan **27** (1969), 290.
3) E. Kusayanagi, T. Kawashima and K. Yamafuji, J. Phys. Soc. Japan **33** (1972), 551.
4) A. Schmid and W. Hauger, J. Low Temp. Phys. **11** (1973), 667.
5) A. I. Larkin, Soviet Phys.-JETP **31** (1970), 784.
6) A. I. Larkin and Yu. N. Ovchinikov, Soviet Phys.-JETP **34** (1972), 651, 1144.
7) H. Raffy, Thèses, Université de Paris-Sud (1972), unpublished.
H. Raffy, J. C. Renard and E. Guyon, Solid State Comm. **11** (1972), 1679.
8) L. P. Gor'kov, Soviet Phys.-JETP **10** (1960), 998.
9) I. O. Kulik and O. Yu. Itskovich, Soviet Phys.-JETP **28** (1969), 102.
10) A. A. Abrikosov, Soviet Phys.-JETP **5** (1957), 1174.
11) V. L. Ginzburg and L. D. Landau, Zhur. Eksp. i Teor. Fiz. **20** (1950), 1064.
12) W. H. Kleiner, L. M. Roth and S. H. Autler, Phys. Rev. **133** (1964), A1226.
13) G. Eilenberger, Phys. Rev. **164** (1967), 628.
14) C. R. Hu and R. S. Thompson, Phys. Rev. **B6** (1972), 110.
15) See for example, Y. B. Kim and M. J. Stephen, chapter 19 in ***Superconductivity*** ed. by R. D. Parks (Marcel Dekker Inc., New York, 1969).
16) H. Raffy, E. Guyon and J. C. Renard, Solid State Comm. **14** (1974), 427, 431.